Hindawi
Advances in Meteorology
Volume 2017, Article ID 1619047, 10 pages
https://doi.org/10.1155/2017/1619047

Research Article

Forest Evapotranspiration and Energy Flux Partitioning Based on Eddy Covariance Methods in an Arid Desert Region of Northwest China

Xiaohong Ma,[1,2,3,4] Qi Feng,[1,2,3] Yonghong Su,[1,2,3] Tengfei Yu,[1,2,3] and Hua Jin[1,2,3,4]

[1]*Northwest Institute of Eco-Environment and Resources, CAS, Lanzhou 730000, China*
[2]*Key Laboratory of Eco-Hydrology of Inland River Basin, CAS, Lanzhou 730000, China*
[3]*Alxa Desert Eco-Hydrology Experimental Research Station, Lanzhou 730000, China*
[4]*University of Chinese Academy of Sciences, Beijing 100049, China*

Correspondence should be addressed to Qi Feng; qifeng@lzb.ac.cn

Received 17 February 2017; Revised 29 April 2017; Accepted 15 May 2017; Published 12 June 2017

Academic Editor: James Cleverly

In this study, the characteristics of energy flux partitioning and evapotranspiration of *P. euphratica* forests were examined in the extreme arid region of Northwest China. Energy balance closure of the ecosystem was approximately 72% ($H + \mathrm{LE} = 0.72 * (R_n\text{-}G) + 7.72$, $r^2 = 0.79$, $n = 12095$), where R_n is the net radiation, G is the soil heat flux, H is the sensible heat flux, and LE is the latent heat flux. LE was the main term of energy consumption at annual time scale because of higher value in the growing season. The ratios of the latent (LE) and sensible (H) heat fluxes to net radiation were 0.47 and 0.28 throughout the year, respectively. Moreover, the yearly evapotranspiration of *P. euphratica* forests was 744 mm year^{-1}. And the mean daily ET was 5.09 mm·d^{-1} in the vibrant growing season. In particular, a small spike in the actual evapotranspiration distribution occurred during the soil ablation period due to the higher temperature and sufficient soil moisture associated with soil thawing. This period is accompanied by a series of physical processes, such as moisture transfer and heat exchange.

1. Introduction

The Ejina oasis is located at the interface between the Alxa highland and desert in the lower reach of Heihe River Basin. This area exhibits a dry climate, harsh natural conditions, and a fragile ecology, and the region is highly vulnerable to climate change. Thus, the sound and steady progress of the Ejina oasis will aid in the prevention of further desertification and help maintain ecological security for the entire Heihe River Basin. Water is the key ecological factor in the inland river basin-oasis ecological processes. In semiarid ecosystems, evapotranspiration (ET) generally represents the greatest flux of water out of an ecosystem, and the relative partitioning of ET between plant and soil surfaces is controlled by water supply and available energy for ET, as well as the path resistance and capacitance along the water travel path [1]. Furthermore, the partitioning between ecosystem latent (LE) and sensible (H) heat fluxes is critical in determining the hydrological cycle, boundary layer development, weather, and climate [2]. A full understanding of the variability of partitioning across different climates and ecosystems and the mechanisms for this variability are necessary. Therefore, an in-depth study of energy flux partitioning and evapotranspiration in a desert riparian *P. euphratica* forest ecosystem is needed to increase the efficiency of water distribution and management in the Heihe River Basin and thereby aid the rational development of the oasis.

Natural vegetation in arid areas plays an essential role in the conservation of biodiversity and reduction of desertification [3]. The natural forest of the study area is dominated by *P. euphratica*. This is a light-demanding species that grows along rivers and represents a component of the natural desert forest ecosystems in China and Middle Eastern countries [4]. The growth of this species is dependent on the groundwater table, which is determined by the amount of water transfer in hyperarid regions. Of course, increased

delivery of water downstream is beneficial. However, water shortage and overexploitation of water as well as conflicts between water demand and supply exist over the entire extent of the Heihe River Basin. The amount and time of ecological water conveyance need to be ensured according to the ecohydrological requirements. Thus, understanding the processes of energy flux partitioning and evapotranspiration of *P. euphratica* forests in different growth stages and their response to anthropogenic and natural disturbances (e.g., drought events, rain pulses, and irrigation) is of foremost importance to ecosystem restoration and estimation of catchment water balance.

The eddy covariance method, a micrometeorological technique, has been widely used to study exchanges of carbon dioxide, water vapor, and energy between the biosphere and atmosphere. Many of these studies have concentrated on the mass and energy exchange between forest ecosystems and atmosphere, such as tropical forests [5, 6], temperate forests [7–9], and boreal forests [10–12]. In addition, several studies were conducted in endemic forest ecosystems, for instance, bamboo forests [13], olive trees [14–16], riparian woodland [17, 18], and mangrove forest [19]. Nevertheless, few studies have used the eddy covariance method to measure the energy and water exchange between desert riparian *P. euphratica* forest and the atmosphere in hyperarid regions. For example, Yuan et al. (2015) reported that evapotranspiration controlled by vegetation phenological characteristics was mainly partitioned to plant transpiration and that groundwater was the main water source as well as the key factor controlling the water cycle process of the desert riparian forest in the lower Tarim River Basin [18]. However, the characteristics of the energy flux partitioning and evapotranspiration of the *P. euphratica* forest are still unclear for different phenophases and areas. These topics require intensive study. The objectives of this research are as follows: to study the characteristics and differences of diurnal variation in energy flux partitioning at different phenological phases in a desert riparian *P. euphratica* forest; to analyze the patterns of seasonal variation in evapotranspiration and crop coefficients in the *P. euphratica* forest; to determine the contribution of latent (LE) and sensible (H) heat fluxes to the available energy of the *P. euphratica* forest in 2014; to identify the evapotranspiration at different phenological phase and total yearly evapotranspiration.

2. Materials and Methods

2.1. Site Description. The study site is dominated by *P. euphratica* and is located in the lower basin of the Heihe River (101°7′25″E, 41°59′34″N) within the continental arid zone (Figure 1), where terrain was relatively regular with highly homogenous land surface cover. The values of the roughness length, zero-displacement height, and site's slope were 1.38 m, 7.9 m, and 0.51 degrees, respectively. The study of the energy flux partitioning and evapotranspiration was conducted throughout the year of 2014. This period was then divided into six subperiods for further investigation. The climate at the site is a typical temperate continental climate, and it can also be classified as an extremely arid climate. The yearly potential evapotranspiration is approximately 2062 mm, while the rainfall is less than 35 mm. According to the data provided by the China Meteorological Data Sharing Service System (Climatic Data Center, National Meteorological Information Center, China Meteorological Administration, Beijing, China) for 1960–2012, the annual mean temperature is 9°C and the annual mean rainfall is 33.24 mm, with 60% of the rainfall occurring during June–October. The soil is derived from fluvial sediments mixed with gray-brown desert deposits [20]. The soil exhibits high salinity as well as low organic matter and nutrient content. The riparian forest is composed of broad-leaved *P. euphratica* and extensive thickets of *T. ramosissima*.

Because of overexploitation of the water resources in the middle reaches of Heihe River beginning in the 1960s, water resources discharged to lower reaches were decreased, which led to degradation of the surrounding ecology [21]. In order to restore the deteriorated ecohydrology in the lower reaches of the Heihe River, the ecological water conveyance project (EWCP) was established in 2002, and water resources have since been under strict artificial controls. As a result of this artificial water management, the groundwater level has increased, the vegetation has experienced a favorable change, and most plants can now acquire water access groundwater [22, 23]. The growth and distribution of vegetation were directly affected by groundwater. Besides, the level and the seasonal variation of evapotranspiration were important factors that impacted the amount and time of water conveyance. The time of water conveyance was September 15, 2014.

2.2. Energy Fluxes and Measurement of Environmental Variables. Fluxes of energy and water between the forest and the atmosphere were measured during January 1, 2014, to December 31, 2014, using the eddy covariance (EC) method. The EC system was installed on terrain that was relatively regular with highly homogenous land surface cover. The instruments included a three-dimensional sonic anemometer (CSAT3, Campbell Scientific, Inc., Logan, UT, USA) to measure wind speed and air temperature and an open-path CO_2/H_2O infrared gas analyzer (LI-7500, LI-COR Inc., Lincoln, NE, USA) to measure the water vapor density and carbon dioxide fluctuations, which was installed at 22 m above the ground. Solar radiation components were measured at 20 m above the ground by a 4-Component Net Radiation Sensor (CNR4, Kipp & Zonen, Delft, NL). The turbulence fluxes were recorded by a CR3000 data logger (Campbell Scientific, Logan, UT, USA) at a 10 Hz sampling frequency, and 30-minute block average fluxes were determined. Radiation data was collected with interval set to 10 minutes. In addition, air temperature and relative humidity were measured at 10 m and 28 m above the ground. Three soil heat flux plates were buried at 6 cm below the soil surface to measure soil heat flux. All these meteorological data were recorded by a CR1000 (Campbell Scientific, Logan, UT, USA).

2.3. Data Processes and Gap Filling. The half-hour sensible (H) and latent (LE) heat fluxes were calculated by Eddypro software following the standard quality control

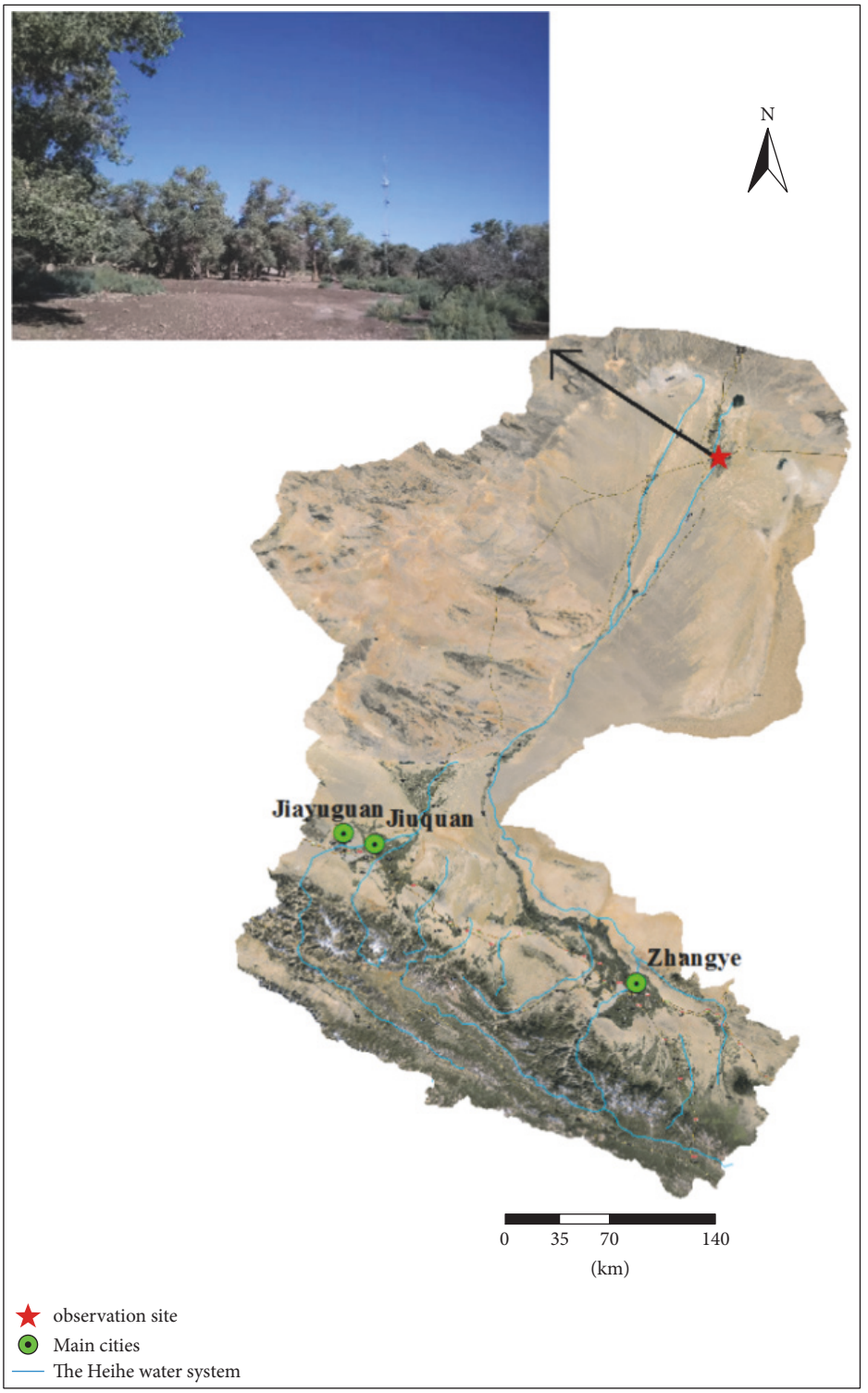

Figure 1: Location and photograph of observation site.

procedures including despiking, 2D coordinate rotation, time lag removal, frequency response correction using model spectra and transfer functions [24], and air density correction [25].

Data gaps (not exceeding two hours) were filled using linear interpolation. Large gaps in energy flux data were replaced with average values calculated using lookup table methods with assorted meteorological conditions [26, 27].

Then, mean diurnal variations (hourly averages binned over periods of 15 days) were used to fill residual gaps.

2.4. Calculations and Statistical Analysis. Surface hourly evapotranspiration of the desert riparian *P. euphratica* forest was calculated as follows:

$$\mathrm{ET} = \frac{\mathrm{LE}}{L\rho_w}, \quad (1)$$

where LE is the latent heat flux ($\mathrm{MJ{\cdot}m^{-2}{\cdot}h^{-1}}$); L is the latent heat of vaporization of water ($2.45\ \mathrm{kJ{\cdot}g^{-1}}$); ρ_w is water density ($1\ \mathrm{g{\cdot}cm^{-3}}$).

The FAO Penman-Monteith method to estimate daily reference evapotranspiration ($\mathrm{mm{\cdot}d^{-1}}$) can be derived:

$$\mathrm{ET}_0 = \frac{0.408\Delta\left(R_n - G\right) + \gamma\left(900/\left(T + 273\right)\right)u_2\left(e_s - e_a\right)}{\Delta + \gamma\left(1 + 0.34u_2\right)}, \quad (2)$$

where ET_0 is reference evapotranspiration [$\mathrm{mm{\cdot}day^{-1}}$]; R_n is net radiation at the crop surface [$\mathrm{MJ{\cdot}m^{-2}{\cdot}day^{-1}}$]; G is soil heat flux density [$\mathrm{MJ{\cdot}m^{-2}{\cdot}day^{-1}}$]; T is mean daily air temperature at 2 m height [°C]; u_2 is wind speed at 2 m height [$\mathrm{m{\cdot}s^{-1}}$]; e_s is saturation vapor pressure [kPa]; e_a is actual vapor pressure [kPa]; Δ is slope vapor pressure curve [$\mathrm{kPa{\cdot}{^\circ}C^{-1}}$]; and γ is the psychrometric constant [$\mathrm{kPa{\cdot}{^\circ}C^{-1}}$].

Thus, the crop coefficient of *P. euphratica* can be calculated as follows:

$$K_c = \frac{\mathrm{ET}}{\mathrm{ET}_0}, \quad (3)$$

where ET and ET_0 are the actual and reference evapotranspiration, respectively.

The evaporative fraction (EF) is a derived variable to describe the partition of available energy into the sensible and latent heat fluxes. The EF was nearly constant during daytime and could be substituted by the midday (10:00–16:00) EF [28, 29]. The EF was calculated by the following equation [30]:

$$\mathrm{EF} = \frac{\mathrm{LE}}{(H + \mathrm{LE})}, \quad (4)$$

where LE is latent heat fluxes and H is the sensible heat fluxes.

3. Results and Discussion

3.1. Meteorological Conditions. In order to study the water and energy exchange between the *P. euphratica* forest and the atmosphere, it is necessary to understand the seasonality of local key environmental variables. Seasonal variations in air temperature (T_a), photosynthetic active radiation (PAR), soil temperature (T_s), potential evapotranspiration (EVP), vapor pressure deficit (VPD), soil volumetric water content (θ_v), and precipitation are presented in Figure 2.

The maximum and minimum value of PAR were 1109.98 $\mu\mathrm{mol{\cdot}m^{-2}{\cdot}s^{-1}}$ (July 3) and 127.83 $\mu\mathrm{mol{\cdot}m^{-2}{\cdot}s^{-1}}$ (October 3), respectively. The PAR showed significant day-to-day fluctuations due to frequent cloud cover, except in winter. In addition, the minimum and maximum daily average air temperature (T_a) at 28 m above the ground were −14.32 (January 8) and 31.29°C (July 16), respectively. Mean annual T_a was 10.83°C with winter average of −7.11°C and summer average of 24.98°C. The mean annual VPD was 1.35 kPa, and VPD winter and summer averages were 0.27 and 2.52 kPa, respectively. The obvious seasonal variation of soil temperature (T_s) at 0, 2, and 4 cm depths was similar to that of T_a. Annual precipitation was 16.4 mm in 2014, and most of the precipitation during 2014 was concentrated in the vibrant growing season. The seasonal variation of θ_v was small, and the value of θ_v was less than 4% throughout the year excluding precipitation days. In other words, the top-soil (upper 5 cm) was dry on nonprecipitation days, and the fluctuation of top-soil volumetric water content was dependent on the precipitation.

3.2. Seasonal and Diurnal Patterns in Energy Balance Components

3.2.1. Diurnal Patterns in Energy Balance Components at Each Stage. Because of the distinct differences found in the energy partitioning pattern and plant phenology, we divided the year into six periods: (a) the soil-frozen period (days of year (DOY) 323–64); (b) the soil ablation period (DOY 65–130); (c) the germination, flowering, and leaf expansion period (DOY 131–169); (d) the vibrant growing season (DOY 170–253); (e) the leaf senescence period including coloration and defoliation stages (DOY 254–288); and (f) the early soil-frozen period (DOY 289–322). The values of energy balance components and environmental variables were distinct for the different periods (Table 1).

Figure 3 shows the diurnal variation in the ensemble half-hourly means of R_n, LE, H, and G during each period at the study site. The daily maximum of R_n during each period was 380.72 $\mathrm{W{\cdot}m^{-2}}$, 515.79 $\mathrm{W{\cdot}m^{-2}}$, 576.28 $\mathrm{W{\cdot}m^{-2}}$, 632.63 $\mathrm{W{\cdot}m^{-2}}$, 547.05 $\mathrm{W{\cdot}m^{-2}}$, and 407.53 $\mathrm{W{\cdot}m^{-2}}$ for the first to the sixth stages, respectively. The magnitude and scope of variation of LE were distinct in each period. LE showed evident variance at each period with values ranging from −2.96 to 24.96 $\mathrm{W\,m^{-2}}$, 0.33 to 50.78 $\mathrm{W\,m^{-2}}$, 3.94 to 106.05 $\mathrm{W\,m^{-2}}$, 5.25 to 160.68 $\mathrm{W\,m^{-2}}$, 17.43 to 218.13 $\mathrm{W\,m^{-2}}$, and 22.02 to 360.52 $\mathrm{W\,m^{-2}}$ in the soil-frozen period, the early soil-frozen period, the soil ablation period, the leaf senescence period, the germination, flowering, and leaf expansion period, and the vibrant growing season, respectively. In addition, the magnitude and scope of H were largest in the soil ablation period, and the value of H ranged from −34.11 to 309.77 $\mathrm{W{\cdot}m^{-2}}$. The value of H ranged from −35.94 to 174.20 $\mathrm{W{\cdot}m^{-2}}$, −34.11 to 309.77 $\mathrm{W{\cdot}m^{-2}}$, −43.11 to 268.24 $\mathrm{W{\cdot}m^{-2}}$, −41.89 to 157.64 $\mathrm{W{\cdot}m^{-2}}$, −38.66 to 209.22 $\mathrm{W{\cdot}m^{-2}}$, and −45.04 to 189.51 $\mathrm{W{\cdot}m^{-2}}$ for the first to the sixth stage, respectively. Moreover, the maximum value of latent heat flux was approximately 360 $\mathrm{W{\cdot}m^{-2}}$ in the vibrant growing season, while the maximum sensible heat flux of 310 $\mathrm{W{\cdot}m^{-2}}$ occurred in the soil ablation period. The sensible heat flux at night was negative in each period and the result

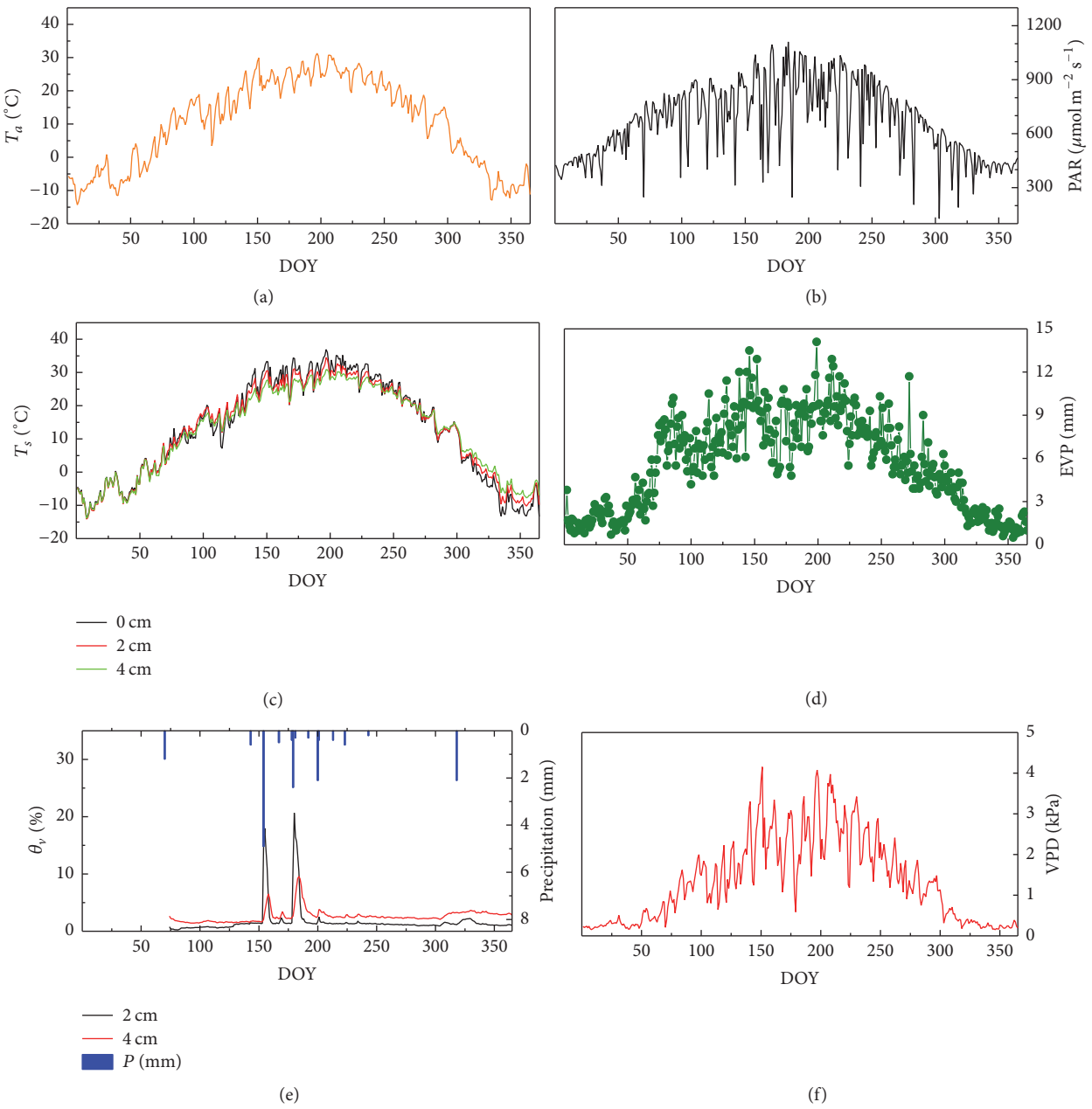

FIGURE 2: Seasonal variation of daily average air temperature (T_a), daily average photosynthetic active radiation (PAR), daily average soil temperature (T_s), daily average potential evapotranspiration (EVP), daily average vapor pressure deficit (VPD), daily average soil volumetric water content (θ_v), and daily total precipitation (P).

was consistent with other findings [31]. In contrast, the latent heat flux was positive at night during the growing season. Si et al. (2015) reported that significant stomatal opening persists during the night in *P. euphratica* forests, leading to the occurrence of substantial water losses, and nighttime sap flow was observed during the whole growing season [20]. This indicated that tree transpiration may have occurred during the night and can explain why the latent heat flux was positive in our study. The midday half-hourly value of H was higher than that of LE in each period, except the vibrant growing season. During the daytime, the value of H was higher than LE in the nongrowing season, was lower than LE in the vibrant growing season, and was lower than LE before or after the midday in the pregrowing season and senescence periods.

3.2.2. Seasonal Variation in Energy Balance Components. The seasonal variation of daily half-hourly means of R_n, LE, H, and G is shown in Figure 4. R_n exhibited significant seasonal and day-to-day variation, ranging from 12 W·m^{-2} (November 26) to 261 W·m^{-2} (July 3). R_n was mostly converted into LE in the growing season (DOY 131–288). The seasonal variation of

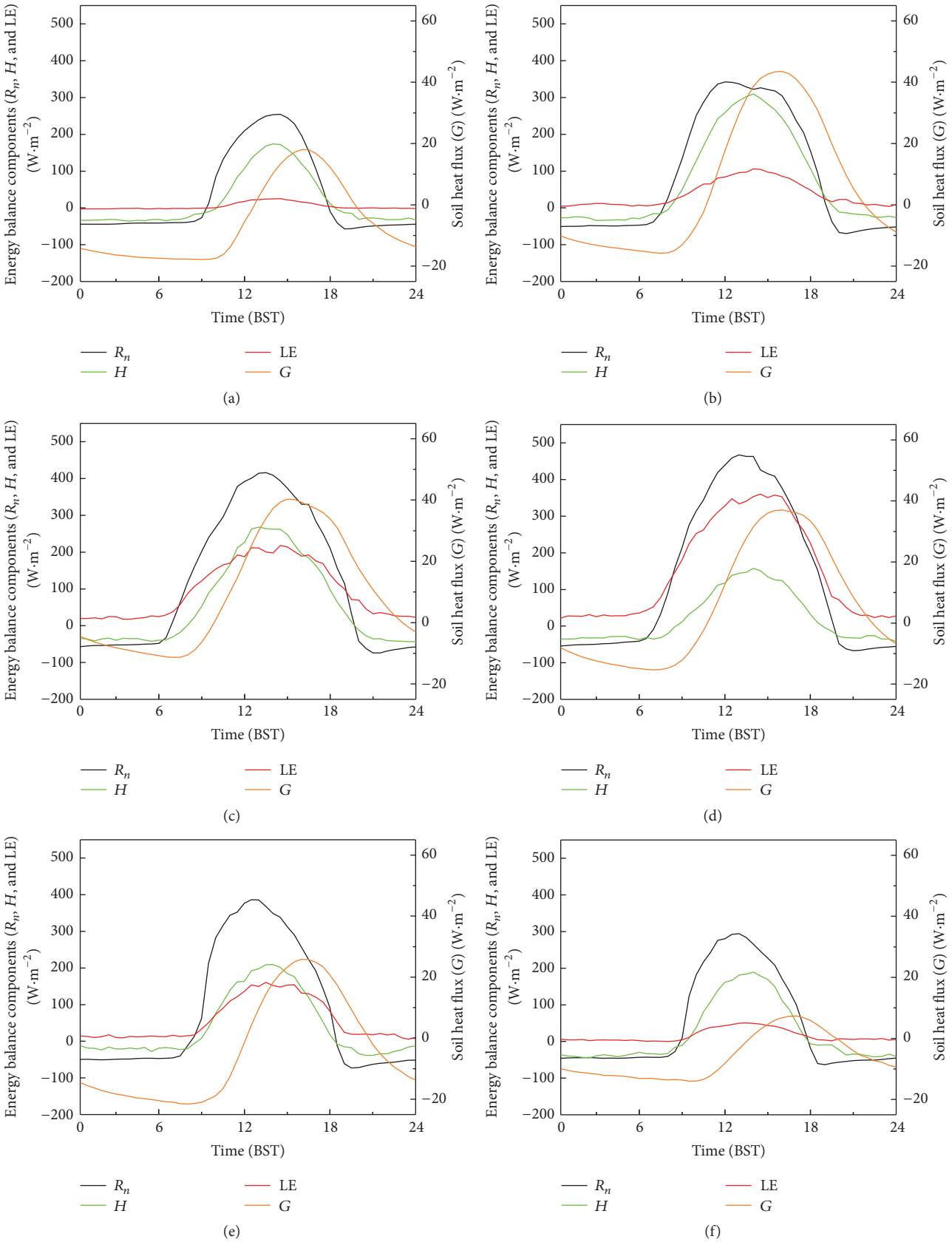

Figure 3: Averaged diurnal variations of net radiation flux (R_n), latent heat flux (LE), sensible heat flux (H), and soil heat flux (G) in the following periods: (a) the soil-frozen period (DOY 326–64); (b) the soil ablation period (DOY 65–130); (c) the germination, flowering, and leaf expansion period (DOY 131–169); (d) the vibrant growing season (DOY 170–253); (e) the leaf senescence period (DOY 254–288); and (f) the early soil-frozen period (DOY 289–322).

Table 1: Daily means of the energy balance components and major biometeorological factors.

	(a) DOY 323–64	(b) DOY 65–130	(c) DOY 131–169	(d) DOY 170–253	(e) DOY 254–288	(f) DOY 289–322	Whole year
T_a (°C)	−6.52	11.21	21.99	25.14	15.31	6.06	10.28
T_{s4} (°C)	−4.61	12.34	23.58	27.13	18.54	8.65	12.23
θ_{v2} (%)	1.37	0.64	2.90	2.43	1.15	1.21	1.69
θ_{v4} (%)	3.20	1.66	2.39	3.22	2.36	2.65	2.63
RH (%)	31.85	17.48	18.69	27.32	25.31	33.13	26.29
Precipitation (mm) (sum.)	0	1.2	6	7.1	0	2.1	16.4
R_n (W·m^{-2})	63.71	148.48	181.97	185.44	128.66	74.85	126.96
H (W·m^{-2})	17.80	74.91	59.33	21.91	38.90	21.34	35.81
LE (W·m^{-2})	4.52	37.38	96.53	150.78	55.47	15.95	60.05
G (W·m^{-2})	−6.24	6.24	9.46	5.48	−4.16	−6.24	0.63
H/R_n	0.28	0.50	0.33	0.12	0.30	0.29	0.28
LE/R_n	0.07	0.25	0.53	0.81	0.43	0.21	0.47
G/R_n	−0.10	0.04	0.05	0.03	−0.03	−0.08	0.01
EF	0.14	0.25	0.49	0.75	0.44	0.24	0.38
ET (mm)	0.17	1.20	3.40	5.09	1.96	0.56	1.79
ET_0 (mm)	1.42	4.61	7.13	6.81	4.75	2.80	4.30
K_c	0.12	0.26	0.48	0.75	0.41	0.2	0.42

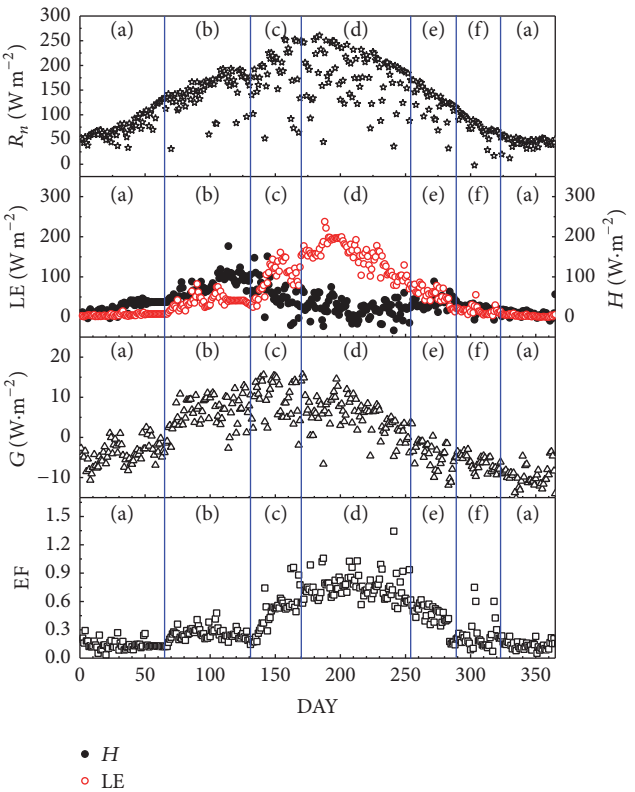

Figure 4: The annual course of daily average net radiation (R_n), latent (LE), sensible (H), and soil heat fluxes, and the evaporative fraction (EF). (a) to (f) represent six periods: (a) the soil-frozen period; (b) the soil ablation period; (c) the germination, flowering, and leaf expansion period; (d) the vibrant growing season; (e) the leaf senescence period; and (f) the early soil-frozen period.

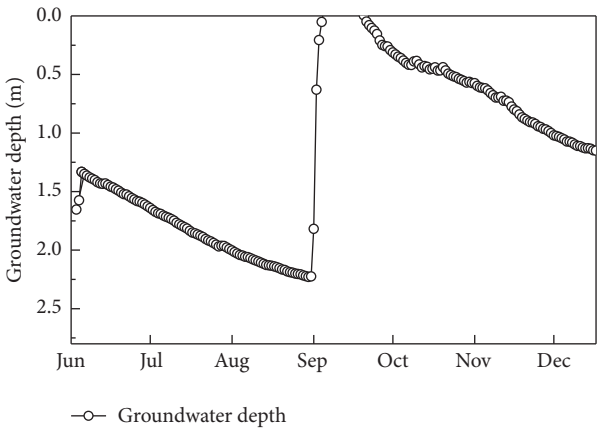

Figure 5: The variation of groundwater depth (m).

LE was distinctly related to plant phenology. And H exhibited reverse course with the LE seasonal course in the growing season. As a result of water regulation on the Heihe River in mid-September, the groundwater level and soil water content increased (Figure 5). Soil freezing and thawing occurred in winter and spring, respectively. Freezing and thawing of soil moisture are accompanied by a series of physical processes, such as moisture transfer and heat exchange. With the start of soil thawing, H and LE increased in the soil ablation period. LE continued to maintain a rapid increase and H tended to decrease during the beginning of the vegetation growth in the germination, flowering, and leaf expansion period. In the vibrant growing season, LE sustained higher values ranging from approximately 150 to 200 W·m^{-2} and H exhibited lower values ranging from approximately −20

to 60 W·m^{-2}. Additionally, LE began to decrease and H started to increase in the leaf senescence period. Over the whole soil-freezing period, H ranged from approximately 0 to 40 W m^{-2} and LE ranged from approximately 0 to 10 W·m^{-2}. For the soil heat flux (G), there was a small yearly cycle in G ranging from approximately −15 to 15 W·m^{-2}. Studying evaporative fraction (EF) plays an important role in interpreting the components of energy budget and evapotranspiration (ET) [28]. Seasonal variation of EF_{midday} was similar to the variation of LE. EF was distinct during different periods, and the mean value of EF was 0.14, 0.25, 0.49, 0.75, 0.44, and 0.24 from the first to sixth stage, respectively (Table 1).

3.3. Energy Balance and Evapotranspiration

3.3.1. Energy Balance Closure. Meteorological data (net radiation, R_n) and soil heat flux (G) are combined with the EC data (sensible and latent heat fluxes, H and LE) to analyze the energy balance closure. H and LE were obtained from EC data, R_n was measured by a Net Radiation Sensor and G was measured at 6 cm below the soil surface by three soil heat flux plates. The result of energy balance closure was determined by a linear regression method using 30 min averaged fluxes. The energy closure of the ecosystem was approximately 72% (H + LE = 0.72 ∗ (R_n-G) + 7.72, r^2 = 0.79, and n = 12095) over the whole study period. Since the ratio of S to net radiation (R_n) was less than 0.4% in the different phenological periods, the energy storage term (S) was neglected in the calculation process. Wilson et al. (2002) comprehensively evaluated energy balance closure across 22 sites and 50 site-years. This assessment indicated [32] a general lack of closure and the slope values ranged from 0.55 to 0.99 with a mean of 0.79 ± 0.01. Thus, the surface energy fluxes (H + LE) are underestimated by approximately 27% relative to estimates of available energy (R_n-G), and the closure value was reasonable for the *P. euphratica* forest ecosystem. The energy balance closure in our study (72%) agreed with an eddy covariance based estimate of riparian forest (*Populus fremontii* S. Watson) in the western US, which was 75% [33], but was lower than the value estimated of riparian forest (*Tamarix ramosissima*) in other desert regions of Northwest China, which was 84% [18].

There is a general lack of the energy balance closure at eddy covariance sites, which could be attributed to several hypotheses [32], including (1) a systematic bias in instrumentation, (2) neglected energy sinks, (3) the loss of low or high frequency contributions to the turbulent flux, (4) neglected advection of scalars, and (5) sampling errors associated with different measurement source areas for terms in energy balance components. In addition, the imbalance of energy could also be caused by neglected energy storage term and biased soil heat flux in this paper. And it was difficult to isolate the contribution of these factors to the lack of energy balance. Heat flux plates have been used widely to measure soil heat flux for their simplicity and durability but suffer from errors such as heat flow distortion and soil-plate contact resistance [34]. What is more, measurement source areas of soil heat flux and other terms in energy balance components do not match. So it is important to improve and calibrate soil heat flux measurement for reducing the imbalance of energy in surface flux measurements.

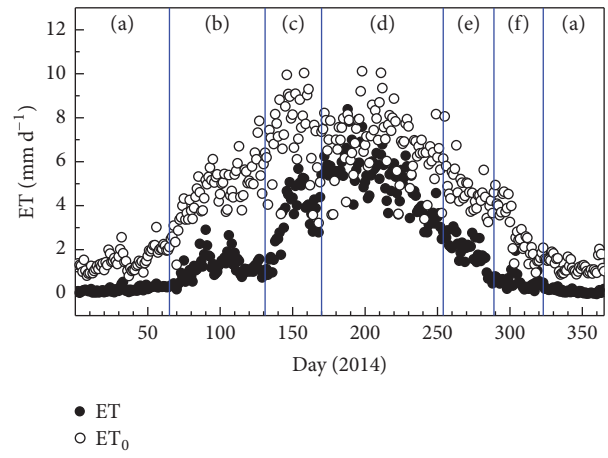

Figure 6: The daily evapotranspiration (ET) and daily reference evapotranspiration (ET_0) in the following periods: (a) the soil-frozen period; (b) the soil ablation period; (c) the germination, flowering, and leaf expansion period; (d) the vibrant growing season; (e) the leaf senescence period; and (f) the early soil-frozen period.

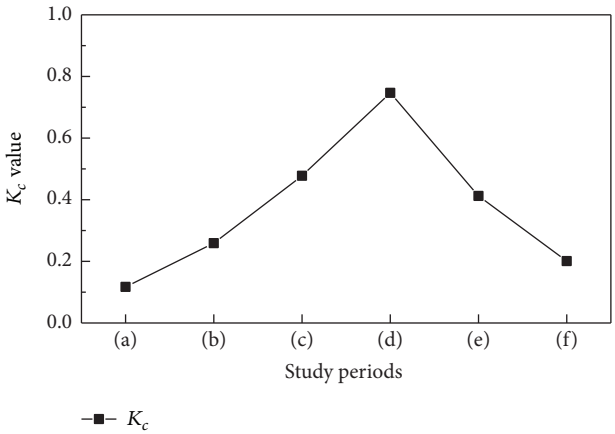

Figure 7: Variation of crop coefficient (K_c) at different study periods.

3.3.2. Seasonal Variation of Evapotranspiration. The seasonal variation of actual evapotranspiration (ET) and reference evapotranspiration (ET_0) of the *P. euphratica* forest is shown in Figure 6 and Table 1. ET and ET_0 exhibited similar seasonal course. The value of ET is much smaller than ET_0 in the soil-freezing season (Figure 7; K_c: 0.12), and averages of ET and ET_0 were 0.17 and 1.42 mm·d^{-1}, respectively. In comparison, K_c was high (K_c: 0.75) in the vibrant growing season, and averages of ET and ET_0 were 5.09 and 6.81 mm·d^{-1}, respectively. The daily ET over the *P. euphratica* forest observation site exhibited distinct variation at different stages of growth. ET began to increase rapidly from approximately 1 mm·d^{-1} in early May to 5 mm·d^{-1} in mid-June during the germination,

flowering, and leaf expansion of the *P. euphratica* forest. ET then fluctuated between approximately 4 mm·d^{-1} and 7 mm·d^{-1} according to the weather and reached its peak (8.38 mm·d^{-1}) on July 7. Afterwards, ET dropped rapidly until the end of November, from 3 mm·d^{-1} to 0.6 mm·d^{-1}. However, a small spike in the ET distribution occurred during the ablation period due to the higher temperature and increased water level associated with soil thawing. During the growing season (DOY 131–288), ET was 628.6 mm·year^{-1}; otherwise ET was 744.4 mm·year^{-1} over an entire year. Plant transpiration accounted for most of the ET with weak soli evaporation for the following reason. ET was much less than ET_0 in the nongrowing season when plant transpiration stopped, indicating that soil evaporation was weak.

The mean daily ET was 5.09 mm·d^{-1} over *P. euphratica* stand during the vibrant growing season in our study. This was similar to results in other desert regions of Northwest China, with a mean value of 4.52 mm·d^{-1} [18]. And cumulative ET was 744.4 mm·year^{-1} over the whole year. The magnitude of the annual cumulative ET is less than that observed over the riparian forest (*Populus fremontii* S. Watson) in the US, where yearly ET was 1095 mm [33, 35]. These differences may be caused by two reasons. First, there was the difference in vegetation coverage at two study sites. The stand density index of the *P. euphratica* stand observed in our study (148 trees per hectare) was less than what is observed in the western US (430 trees per hectare). Second, the soil evaporation was different at two study sites. Our study was conducted in the hyperarid region, where precipitation was less than 35 mm. In contrast, precipitation over the riparian forest (*Populus fremontii* S. Watson) in the US (463 mm) was more, so that the soil evaporation was more strong.

4. Conclusions

Energy balance partitioning and evapotranspiration of a *P. euphratica* forest in an extreme arid region were analyzed using EC method. Several conclusions can be drawn from this study. In summary, we found that the seasonal processes of energy balance partitioning and evapotranspiration of a *P. euphratica* forest were distinctly related to plant phenology in an extreme arid region. The energy balance closure was approximately 72% over the study period and agreed with results estimated from other eddy covariance measurements of riparian forest. The closure status was higher in the vibrant growing seasons than that in the soil-frozen period. Over the whole year, the ratios of the latent (LE), sensible (H), and soil (G) heat fluxes to net radiation were 0.47, 0.28, and 0.01, respectively. Moreover, characteristics of the energy partitioning were distinct at different stages. In the vibrant growing season, LE sustained higher values ranging from approximately 150 to 200 W·m^{-2} and H exhibited lower values ranging from approximately −20 to 60 W·m^{-2}. Otherwise, R_n was mostly converted into H and LE was weak in the nongrowing season. In addition, the yearly evapotranspiration of *P. euphratica* forest was 744 mm·year^{-1} with a mean of 5.09 mm·d^{-1} in the vibrant growing season. And ET was 629 mm·year^{-1} during the growing season (DOY 131–288). ET over riparian forest from our study site was consistent with that from other desert regions' stand of Northwest China but was less than that from field in the western US. The difference may be caused by distinct soil evaporation and vegetation coverage. In conclusion, features of the energy and water exchanges over desert riparian *P. euphratica* forest were basically consistent with general results of other riparian forest.

Conflicts of Interest

The authors declare that there are no conflicts of interest regarding the publication of this paper.

Acknowledgments

This work was funded by the National Natural Science Foundation of China (no. 31370466, no. 91125002, no. 41401033, and no. 31370467).

References

[1] P. J. Mitchell, E. Veneklaas, H. Lambers, and S. S. O. Burgess, "Partitioning of evapotranspiration in a semi-arid eucalypt woodland in south-western Australia," *Agricultural and Forest Meteorology*, vol. 149, no. 1, pp. 25–37, 2009.

[2] K. Wilson, D. Baldocchi, M. Aubinet et al., "Energy partitioning between latent and sensible heat flux during the warm season at FLUXNET sites," *Water Resources Research*, vol. 38, p. 1294, 2002.

[3] Y. Chen, Z. Pang, Y. Chen et al., "Response of riparian vegetation to water-table changes in the lower reaches of Tarim River, Xinjiang Uygur, China," *Hydrogeology Journal*, vol. 16, no. 7, pp. 1371–1379, 2008.

[4] S. Ferreira, K. Hjernø, M. Larsen et al., "Proteome profiling of *Populus euphratica* Oliv. upon heat stress," *Annals of Botany*, vol. 98, no. 2, pp. 361–377, 2006.

[5] Y. Igarashi, T. Kumagai, N. Yoshifuji et al., "Environmental control of canopy stomatal conductance in a tropical deciduous forest in northern Thailand," *Agricultural and Forest Meteorology*, vol. 202, pp. 1–10, 2015.

[6] W. J. Shuttleworth, J. H. C. Gash, C. R. Lloyd et al., "Eddy correlation measurements of energy partition for Amazonian forest," *Quarterly Journal of the Royal Meteorological Society*, vol. 110, no. 466, pp. 1143–1162, 1984.

[7] D. Baldocchi, "Measuring and modelling carbon dioxide and water vapour exchange over a temperate broad-leaved forest during the 1995 summer drought," *Plant, Cell and Environment*, vol. 20, no. 9, pp. 1108–1122, 1997.

[8] L. Gu, T. Meyers, S. G. Pallardy et al., "Direct and indirect effects of atmospheric conditions and soil moisture on surface energy partitioning revealed by a prolonged drought at a temperate forest site," *Journal of Geophysical Research Atmospheres*, vol. 111, no. 16, Article ID D16102, 2006.

[9] J. B. Wu, Y. L. Jing, D. X. Guan et al., "Controls of evapotranspiration during the short dry season in a temperate mixed forest in Northeast China," *Ecohydrology*, vol. 6, no. 5, pp. 775–782, 2013.

[10] M. A. Arain, T. A. Black, A. G. Barr, T. J. Griffis, K. Morgenstern, and Z. Nesic, "Year-round observations of the energy and water vapour fluxes above a boreal black spruce forest," *Hydrological Processes*, vol. 17, no. 18, pp. 3581–3600, 2003.

[11] D. D. Baldocchi and C. A. Vogel, "Energy and CO_2 flux densities above and below a temperate broad-leaved forest and a boreal pine forest," *Tree Physiology*, vol. 16, no. 1-2, pp. 5–16, 1996.

[12] T. Ohta, A. Kotani, Y. Iijima et al., "Effects of waterlogging on water and carbon dioxide fluxes and environmental variables in a Siberian larch forest, 1998–2011," *Agricultural and Forest Meteorology*, vol. 188, pp. 64–75, 2014.

[13] X. Xu, G. Zhou, S. Liu et al., "Implications of ice storm damages on the water and carbon cycle of bamboo forests in southeastern China," *Agricultural and Forest Meteorology*, vol. 177, pp. 35–45, 2013.

[14] L. Testi, F. Orgaz, and F. Villalobos, "Carbon exchange and water use efficiency of a growing, irrigated olive orchard," *Environmental and Experimental Botany*, vol. 63, no. 1-3, pp. 168–177, 2008.

[15] F. J. Villalobos, O. Perez-Priego, L. Testi, A. Morales, and F. Orgaz, "Effects of water supply on carbon and water exchange of olive trees," *European Journal of Agronomy*, vol. 40, pp. 1–7, 2012.

[16] D. G. Williams, W. Cable, K. Hultine et al., "Evapotranspiration components determined by stable isotope, sap flow and eddy covariance techniques," *Agricultural and Forest Meteorology*, vol. 125, no. 3-4, pp. 241–258, 2004.

[17] R. L. Scott, C. Watts, J. G. Payan et al., "The understory and overstory partitioning of energy and water fluxes in an open canopy, semiarid woodland," *Agricultural and Forest Meteorology*, vol. 114, no. 3-4, pp. 127–139, 2003.

[18] G. Yuan, Y. Luo, M. Shao, P. Zhang, and X. Zhu, "Evapotranspiration and its main controlling mechanism over the desert riparian forests in the lower Tarim River Basin," *Science China Earth Sciences*, vol. 58, no. 6, pp. 1032–1042, 2015.

[19] S. Wafar, A. G. Untawale, and M. Wafar, "Litter fall and energy flux in a mangrove ecosystem," *Estuarine, Coastal and Shelf Science*, vol. 44, no. 1, pp. 111–124, 1997.

[20] J. H. Si, Q. Feng, T. F. Yu, and C.-Y. Zhao, "Nighttime sap flow and its driving forces for *populus euphratica* in a desert riparian forest, northwest China," *Journal of Arid Land*, vol. 7, no. 5, article A002, pp. 665–674, 2015.

[21] Q. Guo, Q. Feng, and J. Li, "Environmental changes after ecological water conveyance in the lower reaches of Heihe River, northwest China," *Environmental Geology*, vol. 58, no. 7, pp. 1387–1396, 2009.

[22] P. Wang, Y. Zhang, J. Yu, G. Fu, and F. Ao, "Vegetation dynamics induced by groundwater fluctuations in the lower Heihe River Basin, northwestern China," *Journal of Plant Ecology*, vol. 4, no. 1-2, pp. 77–90, 2011.

[23] Y. Wang, Q. Feng, L. Chen, and T. Yu, "Significance and effect of ecological rehabilitation project in inland river basins in Northwest China," *Environmental Management*, vol. 52, no. 1, pp. 209–220, 2013.

[24] C. J. Moore, "Frequency response corrections for eddy correlation systems," *Boundary-Layer Meteorology*, vol. 37, no. 1-2, pp. 17–35, 1986.

[25] E. K. Webb, G. I. Pearman, and R. Leuning, "Correction of flux measurements for density effects due to heat and water vapour transfer," *Quarterly Journal Royal Meteorological Society*, vol. 106, no. 447, pp. 85–100, 1980.

[26] E. Falge, D. Baldocchi, R. Olson et al., "Gap filling strategies for long term energy flux data sets," *Agricultural and Forest Meteorology*, vol. 107, no. 1, pp. 71–77, 2001.

[27] D. Baldocchi, E. Falge, L. Gu et al., "FLUXNET: a new tool to study the temporal and spatial variability of ecosystem-scale carbon dioxide, water vapor, and energy flux densities," *Bulletin of the American Meteorological Society*, vol. 82, no. 11, pp. 2415–2434, 2001.

[28] S. Li, S. Kang, F. Li, L. Zhang, and B. Zhang, "Vineyard evaporative fraction based on eddy covariance in an arid desert region of Northwest China," *Agricultural Water Management*, vol. 95, no. 8, pp. 937–948, 2008.

[29] W. Shuttleworth, R. Gurney, A. Hsu, and J. Ormsby, *FIFE: The Variation in Energy Partition at Surface Flux Sites*, vol. 186, IAHS Publications, 1989.

[30] A. G. Barr, A. K. Betts, T. A. Black, J. H. McCaughey, and C. D. Smith, "Intercomparison of BOREAS northern and southern study area surface fluxes in 1994," *Journal of Geophysical Research Atmospheres*, vol. 106, no. 24, Article ID 2001JD900070, pp. 33543–33550, 2001.

[31] Z. Gaofeng, L. Ling, S. Yonghong et al., "Energy flux partitioning and evapotranspiration in a sub-alpine spruce forest ecosystem," *Hydrological Processes*, vol. 28, no. 19, pp. 5093–5104, 2014.

[32] K. Wilson, A. Goldstein, E. Falge et al., "Energy balance closure at FLUXNET sites," *Agricultural and Forest Meteorology*, vol. 113, no. 1–4, pp. 223–243, 2002.

[33] J. Kochendorfer, E. G. Castillo, E. Haas, W. C. Oechel, and U. K. T. Paw, "Net ecosystem exchange, evapotranspiration and canopy conductance in a riparian forest," *Agricultural and Forest Meteorology*, vol. 151, no. 5, pp. 544–553, 2011.

[34] X. Peng, J. Heitman, R. Horton, and T. Ren, "Field evaluation and improvement of the plate method for measuring soil heat flux density," *Agricultural and Forest Meteorology*, vol. 214-215, pp. 341–349, 2015.

[35] C. N. Dahm, J. R. Cleverly, J. E. A. Coonrod, J. R. Thibault, D. E. Mcdonnell, and D. J. Gilroy, "Evapotranspiration at the land/water interface in a semi-arid drainage basin," *Freshwater Biology*, vol. 47, no. 4, pp. 831–843, 2002.